ORGANIC LETTERS

2013
Vol. 15, No. 19
4976–4979

Kinetic Stabilization of *N*,*N*-Dimethyl-2-propyn-1-amine *N*-Oxide by Encapsulation

Albano Galán,[†] Guzmán Gil-Ramírez,[†] and Pablo Ballester*[,†,‡]

Institute of Chemical Research of Catalonia (ICIQ), Avgda. Països Catalans 16, 43007 Tarragona, Spain, and Catalan Institution for Research and Advanced Studies (ICREA), Passeig Lluís Companys, 23, 08018 Barcelona, Spain

pballester@iciq.es

Received August 6, 2013

ABSTRACT

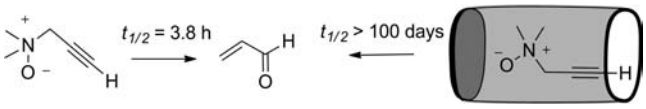

Thermally and in nonprotic media *N*,*N*-dimethyl-2-propyn-1-amine *N*-oxide undergoes two consecutive sigmatropic rearrangements affording propenal. Two molecular containers capable of the quantitative inclusion/encapsulation of the *N*-oxide are described. The *N*-oxide becomes kinetically stabilized when included in the containers. The relationship between the observed kinetic stabilization of the *N*-oxide and the thermodynamic and kinetic stability of its inclusion complexes is explained and modeled.

In recent years, different types of synthetic molecular containers have been developed as mimics of protein binding sites, antibodies, and enzymes.[1−3] Molecular containers are molecules or supramolecules able to reproduce some of the properties exhibited by their biological counterparts. These properties include the reversible inclusion/encapsulation of molecular guests within their internal cavities, the isolation of the included guests from the bulk solvent, and the selection of guests on the basis of host−guest complementarity in size, shape, and functional groups. In relevant examples, synthetic molecular containers can efficiently promote chemical reactions of encapsulated[4,5] and coencapsulated substrates,[6,7] altering the typical regio- and/or stereochemical outcome of the reactions free in solution.[8,10] They can also kinetically stabilize highly reactive intermediates[9] or substrates,[11] bind guests in high energy conformations,[12−15] as well as modify the catalytic properties of encapsulated organometallic complexes.[16,17] In this communication, we describe a significant kinetic stabilization of the *N*,*N*-dimethyl-2-propyn-1-amine *N*-oxide, **1a**, achieved by supramolecular inclusion in two different molecular containers. We also present a simple kinetic model that quantitatively relates the observed kinetic stabilization with the thermodynamic/kinetic stability of the inclusion complexes (Scheme 1). The reported

[†] Institute of Chemical Research of Catalonia.
[‡] Catalan Institution for Research and Advanced Studies.

(1) Yoshizawa, M.; Klosterman, J. K.; Fujita, M. *Angew. Chem., Int. Ed.* **2009**, *48*, 3418–3438.
(2) Breiner, B.; Clegg, J. K.; Nitschke, J. R. *Chem. Sci.* **2011**, *2*, 51–56.
(3) Wiester, M. J.; Ulmann, P. A.; Mirkin, C. A. *Angew. Chem., Int. Ed.* **2011**, *50*, 114–137.
(4) Fiedler, D.; van Halbeek, H.; Bergman, R. G.; Raymond, K. N. *J. Am. Chem. Soc.* **2006**, *128*, 10240–10252.
(5) Hooley, R. J.; Rebek, J., Jr. *Org. Biomol. Chem.* **2007**, *5*, 3631–3636.
(6) Horiuchi, S.; Murase, T.; Fujita, M. *Chem.—Asian J.* **2011**, *6*, 1839–1847.
(7) Kang, J. M.; Hilmersson, G.; Santamaria, J.; Rebek, J., Jr. *J. Am. Chem. Soc.* **1998**, *120*, 3650–3656.
(8) Hastings, C. J.; Backlund, M. P.; Bergman, R. G.; Raymond, K. N. *Angew. Chem., Int. Ed.* **2011**, *50*, 10570–10573.
(9) Restorp, P.; Rebek, J., Jr. *J. Am. Chem. Soc.* **2008**, *130*, 11850–11851.
(10) Yoshizawa, M.; Tamura, M.; Fujita, M. *Science* **2006**, *312*, 251–254.
(11) Mal, P.; Breiner, B.; Rissanen, K.; Nitschke, J. R. *Science* **2009**, *324*, 1697–1699.
(12) Breiner, B.; Clegg, J. K.; Nitschke, J. R. *Chem. Sci.* **2011**, *2*, 51–56.
(13) Takezawa, H.; Murase, T.; Fujita, M. *J. Am. Chem. Soc.* **2012**, *134*, 17420–17423.
(14) Korner, S. K.; Tucci, F. C.; Rudkevich, D. M.; Heinz, T.; Rebek, J. *Chem.—Eur. J.* **2000**, *6*, 187–195.
(15) Porel, M.; Jayaraj, N.; Raghothama, S.; Ramamurthy, V. *Org. Lett.* **2010**, *12*, 4544–4547.
(16) Wang, Z. J.; Clary, K. N.; Bergman, R. G.; Raymond, K. N.; Toste, F. D. *Nat. Chem.* **2013**, *5*, 100–103.
(17) Horiuchi, S.; Murase, T.; Fujita, M. *Angew. Chem., Int. Ed.* **2012**, *51*, 12029–12031.

10.1021/ol402236z
Published on Web 09/19/2013

results constitute unique examples of the use of molecular containers in the kinetic stabilization of reactive species, which would otherwise fragment through sigmatropic rearrangements.

Scheme 1. Proposed Mechanism for the Thermal Decomposition of Tertiary Prop-2-ynylic *N*-Oxides **1**

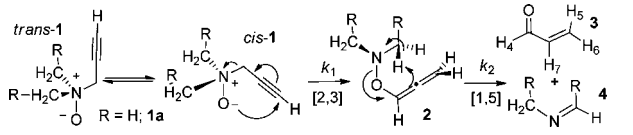

Thermally and in nonprotic media, tertiary propargylamine *N*-oxides undergo a concerted [2,3]-sigmatropic rearrangement to yield *O*-allenyl ethers **2**.[18,19] In turn, these *O*-allenyl ethers are kinetically unstable and experience a rapid elimination, akin to a [1,5]-hydrogen shift, generating propenal **3** and the corresponding Schiff base **4**. The kinetic stability of the intermediate *O*-allenyl ether **2** depends on the substituents on the nitrogen atom.[20]

We hypothesized that the confinement of **1a** in properly inner functionalized molecular containers could reduce or even eliminate its tendency to decompose by increasing the energy difference between bound **1a** and the transition state (TS) leading to the *O*-allenyl ether **2a**, compared to that of the reaction occurring free in solution. Both the formation of hydrogen bonds with the oxygen atom of the *N*-oxide **1a** (reduce oxygen nucleophilicity) and the induction of steric strain in the *cis*-conformation of **1a** (required in the TS) seemed to be good starting points to achieve the goal. Due to the extensive use of aromatic panels to shape the concave cavities of uni- and supramolecular containers, it is synthetically challenging to place polar groups in their interiors.[21,22] In addition, the lack of inner functionalization disfavors the inclusion of polar guests, rendering the selectivity of the encapsulation's process mainly determined by size and shape complementarity. In trying to overcome these limitations, we and others have used aryl-extended calix[4]pyrroles as privileged scaffolds for the construction of unimolecular[23] and supramolecular containers with polar interiors.[24]

We previously reported the efficient inclusion of *N*-oxides in water-soluble "four-wall" aryl-extended calix[4]pyrroles

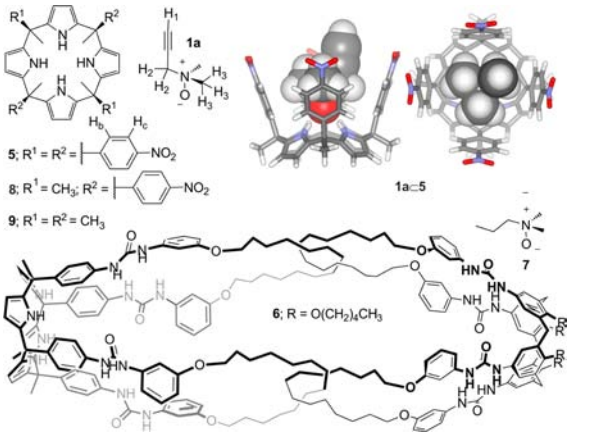

Figure 1. Molecular structures of *N*-oxides **1a** and **7**, containers **5** and **6**, and reference compounds **8** and **9**. Top right: Side and top views of the energy-minimized complex **1a**⊂**5**. Note that **1a** must adopt the *trans*-conformation to fit in the aryl-extended calix[4]pyrrole binding pocket of **5**.

that are structurally related to tetranitro **5** (Figure 1).[25] We demonstrated that *N*-oxides can be encapsulated alone or coencapsulated with a $CHCl_3$ molecule in the mechanically locked capsule **6** (Figure 1).[26] Molecular modeling studies suggested a good match between the *trans*-conformation of **1a** and the size, shape, and functionality of the inner cavities of the calix[4]pyrrole units of containers **5** and **6**. Conversely, the *cis*-conformer of **1a** is not a good fit. Interestingly, *trans*-**1a** forms four hydrogen bonds with the endohedrally directed pyrrole NHs of the calixpyrrole units of the containers. Thus, the included/encapsulated *trans*-**1a** displays the features planned above to alter its inherent reactivity (Figure 1).

The *N*-oxide of *N*,*N*-dimetyl-2-propyn-1-amine, **1a**, was obtained as a white solid in 80% yield from reacting equimolar amounts of *m*-chloroperbenzoic acid and the amine in chloroform solution at 25 °C followed by column chromatography through alumina.[20] *N*-Oxide **1a** was stable for months when stored as a solid in a refrigerator. In contrast, the ^{1}H NMR analysis of a 60 mM dichloromethane solution of **1a** at 298 K provided evidence for the decomposition of the *N*-oxide with the appearance of proton signals characteristic for propenal **3**. The intensity of the proton signals of **3** grew at the expense of those assigned to **1a**. The observation of the proton signals corresponding to **3** indicated (a) that the *O*-allenyl ether intermediate **2a** is not kinetically stable and (b) that the *N*-methylenemethanamine **4a**, a byproduct of the formal [1,5]-hydrogen shift reaction, decomposes rapidly.[27]

^{1}H NMR spectroscopy was used to monitor the decomposition kinetics of a freshly prepared CD_2Cl_2 solution of

(18) Craig, J. C.; Ekwuribe, N. N.; Gruenke, L. D. *Tetrahedron Lett.* **1979**, *20*, 4025–4028.
(19) Khuthier, A. H.; Aliraqi, M. A.; Hallstrom, G.; Lindeke, B. *J. Chem. Soc., Chem. Commun.* **1979**, 9–10.
(20) Hallstrom, G.; Lindeke, B.; Khuthier, A. H.; Aliraqi, M. A. *Tetrahedron Lett.* **1980**, *21*, 667–670.
(21) For recent reviews of inner functionalization of molecular containers, see: (a) Adriaenssens, L.; Ballester, P. *Chem. Soc. Rev.* **2013**, *42*, 3261–3277. (b) Kubik, S. Molecular Cages and Capsules with Functionalized Inner Surfaces. In *Chemistry of Nanocontainers*; Albrecht, M., Hahn, E., Eds.; Springer: Berlin, 2011; Vol. 319, pp 1−34.
(22) Young, M. C.; Johnson, A. M.; Gamboa, A. S.; Hooley, R. J. *Chem. Commun.* **2013**, *49*, 1627–1629.
(23) Park, I. W.; Kim, S. K.; Lee, M. J.; Lynch, V. M.; Sessler, J. L.; Lee, C. H. *Chem.—Asian J.* **2011**, *6*, 2911–2915.
(24) Adriaenssens, L.; Ballester, P. *Chem. Soc. Rev.* **2013**, *42*, 3261–3277.
(25) Verdejo, B.; Gil-Ramirez, G.; Ballester, P. *J. Am. Chem. Soc.* **2009**, *131*, 3178–3179.
(26) Chas, M.; Ballester, P. *Chem. Sci.* **2012**, *3*, 186–191.
(27) Cattoen, X.; Miqueu, K.; Gornitzka, H.; Bourissou, D.; Bertrand, G. *J. Am. Chem. Soc.* **2005**, *127*, 3292–3293.

1a (Figure 2a,b). The ^{1}H NMR spectrum of the solution recorded after 3 h showed the expected proton signals for **3** (δ = 9.6 ppm, CHO, and δ = 6.5 ppm, HC=CH_2) (Figure 2b). We followed the change in the integral values for both the proton signals of *N*-oxide **1a** and propenal **3** during two half-lives. The decomposition process was investigated at three different initial concentrations of **1a** (26, 60, and 120 mM). The experimental kinetic data were fitted, using global multivariate factor analysis and the differential kinetics module implement in SPECFIT,[28] to a reaction model considering the direct conversion of **1a** to **3**. We obtained very good fits of the experimental data, for both the decomposition and formation reactions, at any of the concentrations used (see Supporting Information). The averaged value of the rate constant returned from the fits was $k_{obs} = 5.0 \pm 0.3 \times 10^{-5}\ s^{-1}$. The half-life of *N*-oxide **1a** free in solution is 3.8 ± 0.2 h and, as expected for first-order reactions ($t_{1/2} = 0.693/k_{obs}$), independent of its initial amount. The analysis of the kinetic data assumes that the rate-determining step of the reaction is the [2,3]-sigmatropic rearrangement of **1a** affording the *O*-allenyl ether **2**. This hypothesis is substantiated by the following evidence: (a) the intermediate *O*-allenyl ether **2** is not detected experimentally in the ^{1}H NMR kinetic experiments and (b) the results are obtained from the theoretical investigation of the reaction pathways.[29] The addition of an equimolar amount of **5** to a freshly prepared 2.5 mM CD_2Cl_2 solution of **1a** had a strong impact on the decomposition kinetics. The first half-life of **1a** in the presence of **5** was estimated by simple visual extrapolation of the curves of disappearance of **1a**⊂**5** and formation of **3** as $t_{1/2} > 50$ h. This represents an almost 18-fold increase compared to the kinetic stability of **1a** free in solution. The ^{1}H NMR analysis of the freshly prepared equimolar mixture of **1a** and **5** reveals the quantitative assembly of the **1a**⊂**5** inclusion complex (Figure 2d). We sought to determine the relationship between the observed kinetic stabilization of **1a** and the thermodynamic and kinetic properties of the inclusion complex **1a**⊂**5**.[30] To this end, the kinetic data for the decomposition of **1a** in the presence of **5** were fitted, using the differential kinetics module of SPECFIT, to a model that also considers the reversible formation of the inclusion complex **1a**⊂**5** (Scheme 2). This kinetic model implicitly assumes that the decomposition of **1a** occurs exclusively when the species is free in solution. In order to minimize the number of variables to fit, the value of the rate constant k_1 for the decomposition of free **1a** was fixed to $5.0 \times 10^{-5}\ s^{-1}$. This is the value calculated in the absence of molecular container **5** (vide supra).

(28) SPECFIT/32 from Spectrum Software Associates.

(29) The geometries of the transition states (TS) for each one of the two sequential rearrangements were determined using DFT calculations at the M06-2X/aug-cc-pVDZ level of theory and using a continuum solvation model for CH_2Cl_2. The free energy differences (ΔG^*) with respect to *trans*-**1a** for TS1[2,3] and TS2[1,5] are 24.3 and 22.0 kcal/mol, respectively. TS1 is the rate-determining step, and the rate law obeys $-k_1$[**1**]. The sensible agreement that exists between the theoretical and experimental (23.1 kcal/mol) values determined for ΔG^* supports the identity of $k_1 = k_{obs}$.

(30) The half-life of a substrate depends on its initial concentration for all reactions not following first-order kinetics.

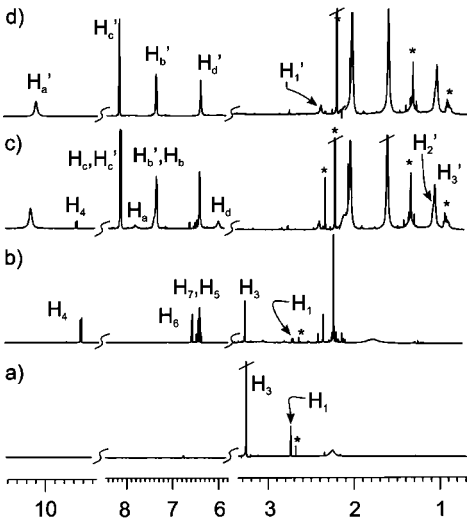

Figure 2. Selected regions of the ^{1}H NMR spectra (500 MHz, 298 K) of (a) a freshly prepared 26 mM CD_2Cl_2 solution of **1a**; (b) a solution of **1a** after 3 h; (c) a solution of **1a** in the presence of 1 equiv of **5** after 13 h; (d) a freshly prepared equimolar solution of **1a** and **5**. See Scheme 1 and Figure 1 for proton assignment. Primed numbers indicate signals of protons bound.

Moreover, complex **7**⊂**5** was employed as an ideal system to derive reference values for the kinetic and thermodynamic properties of **1a**⊂**5**. The 1D ^{1}H NMR spectrum of a CD_2Cl_2 solution of **5** containing 0.5 equiv of *N*-oxide **7** showed separated proton signals for free and bound tetranitro host **5**. In addition, half of the total amount of container **5** is bound, and no proton signals for the free *N*-oxide **7** are detected. These observations indicated that the binding process is slow on the ^{1}H NMR time scale and that the stability constant of the inclusion complex can be estimated at K(**7**⊂**5**) > $10^4\ M^{-1}$. We performed a 2D EXSY experiment on the mixture at 298 K. Using the integration values of the diagonal and cross-peaks, we determined the rate constant for the magnetization exchange between bound and free states of **5** as $k_{-1mag} = 10\ s^{-1}$. This value is directly related to the dissociation rate constant of the **7**⊂**5** complex $k_{off} = k_{-1mag} = 10\ s^{-1}$ and was used to set the value of dissociation rate constant for the **1a**⊂**5** complex in the data fitting.

Scheme 2. Kinetic Model Involving the Formation of the Stabilizing Inclusion Complex **1a**⊂**5**

$$\mathbf{1a} \xrightarrow{k_1} \mathbf{3}\ ;\ \mathbf{1a} + \mathbf{5} \underset{k_{off}}{\overset{k_{on}}{\rightleftharpoons}} \mathbf{1a}\subset\mathbf{5}\ ;\ K(\mathbf{1a}\subset\mathbf{5}) = \frac{k_{on}}{k_{off}}$$

Next, the kinetic data of the supramolecular system **1a**/**5** (changes in concentrations of **3**, **5**, and **1a**⊂**5** species vs time) were analyzed with the kinetic model in Scheme 2, and k_1 and k_{off} were fixed to the above values. The process provided good fits to the experimental data and returned the value of the second-order rate constant for complex

formation, $k_{on} = 1.2 \times 10^5\ M^{-1}\ s^{-1}$, as the only variable to refine. The ratio of formation and dissociation rate constants for the **1a**⊂**5** complex affords its thermodynamic stability constant as K(**1a**⊂**5**) = $1.2 \times 10^4\ M^{-1}$. The calculated value is in very good agreement with the one measured using ITC experiments for the **7**⊂**5** model complex (K(**7**⊂**5**) = $1.3 \pm 0.2 \times 10^4\ M^{-1}$). This result gives clear indication of the quality and fit of the kinetic data analysis used. It also demonstrates that the kinetic stabilization of **1a** in the presence of **5** is not due to the release of **1a** from the container being rate-limiting, but simply to the significant reduction of the concentration of free **1a** in solution.

As long as the release of **1a** from the container is not rate-determining, the kinetic model quantitatively predicts the relationship between the apparent kinetic stabilization of **1a** and the thermodynamic/kinetic stability of the complexes inhibiting decomposition. Thus, control compounds **8** and **9** with K(**7**⊂**8** or **7**⊂**9**) $< 50\ M^{-1}$ proved to be completely inefficient in the kinetic stabilization of **1a** (Supporting Information). Next, we simulated the expected kinetic speciation for propenal **3** from a 0.5 mM equimolar mixture of **1a** and a putative container forming an encapsulation complex with a stability constant 2 orders of magnitude larger than that for **1a**⊂**5** (Supporting Information).[31] The first half-life of **1a** was determined as *45 days* using curve interpolation of the simulated changes in the concentration of **3** versus time (Supporting Information). This represents a significant kinetic stabilization of **1a** when compared to the experimentally measured first half-lives of 3.8 h for 2.5 mM solutions of free **1a** or > 50 h in the presence of 1 equiv of **5**. In short, after 45 days, only 50% of **1a** in solution should have decomposed to propenal **3** if stored (encapsulated) in such molecular container.

N-Oxides **1a** and **7** are also nicely encapsulated in the calix[4]pyrrole hemisphere of the mechanically locked capsule **6**, while the calix[4]arene hemisphere is occupied by one molecule of chloroform (Figure S3).[26,32] The value of K(**7**⊂**6**) was estimated using ITC experiments as $> 1.0 \times 10^6\ M^{-1}$, supporting the suitability of **6** as a molecular flask for extending the first half-life of **1a** in the liquid state. The ^{1}H NMR spectrum of a 0.5 mM CD_2Cl_2 solution containing equimolar amounts of **1a** and **6** shows the characteristic earmarks for quantitative formation of the encapsulation complex **1a**⊂**6** (Figure S2a). The pyrrole NH protons moved downfield (δ = 10.2 ppm; $\Delta\delta$ = 1.6 ppm) as a result of hydrogen bonding interaction between the NHs and the oxygen atom of the *N*-oxide. The protons of the methyl groups for the bound guest appear upfield shifted and resonate as two diastereotopic signals (δ = 0.82 and 0.74 ppm) due to the chiral nature of the container. Even after 2 months, the weekly ^{1}H NMR spectroscopy analysis of the 0.5 mM CD_2Cl_2 solution containing the **1a**⊂**6** complex did not reveal the presence of signals for the protons of **3**.[33] This observation suggests that K(**1a**⊂**6**) should be more than 2 orders of magnitude larger than K(**1a**⊂**5**) (Figure S12). The series of ^{1}H NMR spectra acquired during this time period indicated that the encapsulation complex **1a**⊂**6** remained unaltered in solution (Figure S4). Finally, the decomposition of **1a** into **3** was induced by competitive release from the container (Supporting Information).

In conclusion, we demonstrated that the inherent reactivity of *N*-oxide **1a** affording **3** can be modulated by inclusion/encapsulation in molecular containers. The containers used feature concave, polar interiors based on aryl-extended calix[4]pyrrole scaffolds. *N*-Oxide **1a** is encapsulated in *trans*-conformation and forms four hydrogen bonds between its oxygen atom and the pyrrolic NH protons of the container. We derived a kinetic model that quantitatively explains the relationship between the apparent kinetic stabilization of **1a** and the thermodynamic/kinetic stability of the complexes formed with the molecular flasks. The kinetic stabilization does not result from a rate-determining dissociation of **1a** from the container but simply from the significant reduction of its concentration free in solution in the presence of the molecular containers.

Acknowledgment. We are grateful for funding from Gobierno de España MINECO (CTQ2011-23014), Generalitat de Catalunya DURSI (2009SGR6868), and ICIQ Foundation. A.G. thanks MINECO for a FPU fellowship.

Supporting Information Available. Experimental procedures, ^{1}H NMR experiments, fits of the kinetic data simulations, and ITC experiments. This material is available free of charge via the Internet at http://pubs.acs.org.

(31) The speciation simulations provide identical results independently of the absolute values used for k_{on} and k_{off}, as long as its ratio is maintained constant and equal to $2.0 \times 10^6\ M^{-1}$ and $k_{off} > 5 \times 10^{-5}\ s^{-1}$.

(32) In dichloromethane solution, the chemical exchange between the encapsulated solvent molecule and the bulk solvent molecules is fast on the ^{1}H NMR time scale even at low temperatures.

(33) We estimate that the lower detection limit of our analysis for **3** is 0.2 mM.

The authors declare no competing financial interest.